

# Using Coronal Depth Maps to Detect Identifiable Surface Features on Structural Head Imaging

Konstantinos Sideris, BS<sup>1</sup>, Brian E. Chapman, PhD<sup>2</sup>

<sup>1</sup>University of California, Los Angeles, Los Angeles, CA, USA

<sup>2</sup> University of California, San Diego, San Diego, CA, USA

## Abstract

*Sharing medical images is becoming increasingly crucial for knowledge discovery in medicine and science. An important issue associated with image sharing is the potential for a breach of patient privacy. Prior work has primarily focused on removing identifying metadata such as name, age or sex from image headers. However, there remains the potential for images being identified directly from the image itself. This is particularly true for images of the head. Techniques have been developed previously that remove the entire facial region from the image. This technique is suboptimal in that the radical defacing removes landmarks that may be useful for correlating with other images, but yet are not important for facial recognition. In this paper we present a framework for identifying and removing features from structural head images. Our methodology focuses on geometric features of the face and thus has the potential to be modality independent.*

## Introduction

Sharing medical images with compliance to existing regulations requires that all identifying data be removed. When sharing medical images, all identifying metadata are removed (e.g. patient name) or modified (e.g. returning an age as a decade range) so as to make the metadata HIPAA compliant. While this practice is successful in ensuring anonymity in most cases, in the special case of structural head imaging a good amount of identifying data is contained within the actual image content.

Researchers have proven that a variety of head features can be used to identify a person. The face recognition literature has suggested that internal facial features (i.e. eyes, nose, and mouth) are particularly relevant when recognizing a familiar individual as shown in Bruce et al.<sup>1</sup> This is validated by the extensive computerized facial recognition literature. We refer the reader to the excellent literature overview by Bowyer et al.<sup>2</sup>

Zhang et al. have shown that skull structure matching can be used to identify medical images.<sup>3</sup> It is conceivable that other non-facial features within an image may also be unique and thus identifiable (e.g. gray and white matter patterns of the brain), re-identification of the patient through these features requires an existing identified medical image to be accessible. Facial features, however, may exist within an observer's memory and are ubiquitous in our media saturated culture.

Existing techniques of deidentification have approached the problem by removing the entire facial area. The process of Bischoff-Grethe et al.<sup>4</sup> uses a statistical model of MR images to classify voxels as being face and non-face voxels and then removes the former. Schimke et al.<sup>5</sup> define a plane to cut the surface of the face from the MR image.

In this work we focus on the importance of patient identification through facial features in volumetric renderings of head structural images. We present a methodology to use spatial analysis to localize specific features important for facial recognition. Once these features are localized they may form the basis of a defacing algorithm that simultaneously preserves privacy and minimizes the features that are removed from the image, features that may be useful for subsequent purposes such as correlating with E.E.G. electrode placement.

## Methodology

To develop and evaluate our method, we acquired de-identified, structural MRI images of the head from the ADNI LONI Alzheimer's disease repository (<http://adni.loni.ucla.edu>).<sup>6</sup> Twenty-nine images were processed for this study.

The main idea behind our methodology is to localize the dominant identifying features of a human face in the 2D coronal depth map of the MRI data. A depth map is a 2D image where every pixel value (grayscale) corresponds to the distance between the point of view and that pixel. Using the depth map simplifies our analysis of reducing the

dimensionality from 3D to 2D yet retains the 3D information of the original volumetric image. An additional advantage of this approach is the large amount of prior experience with 2D facial recognition that can be exploited.

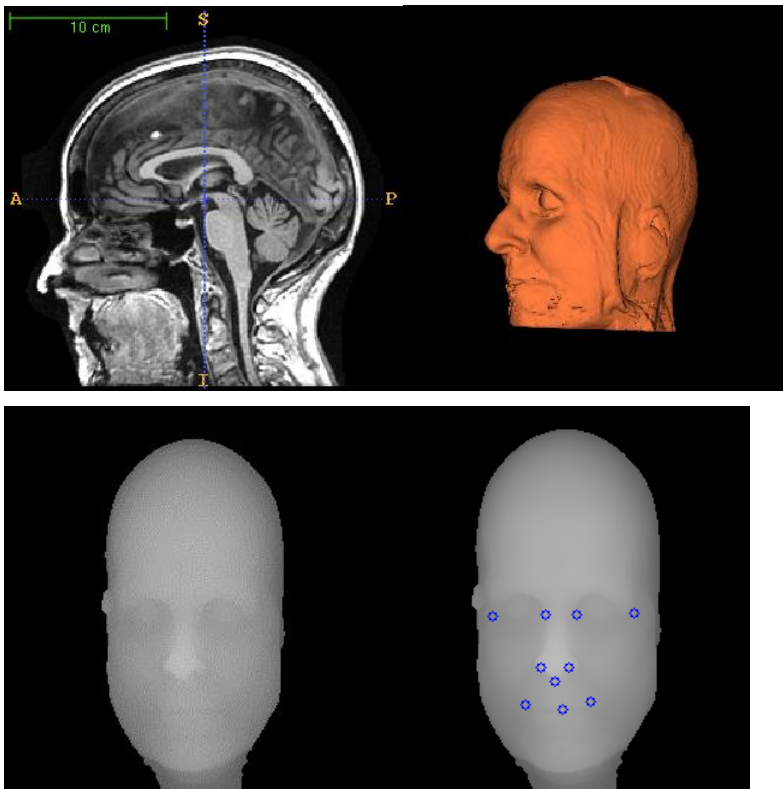


**Figure 1.** Example slice through original MRI image, surface rendering, and coronal depth map.

After the coronal depth map was generated, we then manually annotated the facial features on the images to be used as training samples. For this study, we focused on identifying the eyes, nose, and mouth. For the eyes we marked the left and right boundaries, while for the nose and mouth we marked the left and right boundaries and a center point (bottom of the nose and center for the mouth). Figure 1 shows an example MRI slice (top left), the surface rendering for the corresponding volume (top right), the generated coronal depth map (bottom left) and the manual annotations (bottom right).

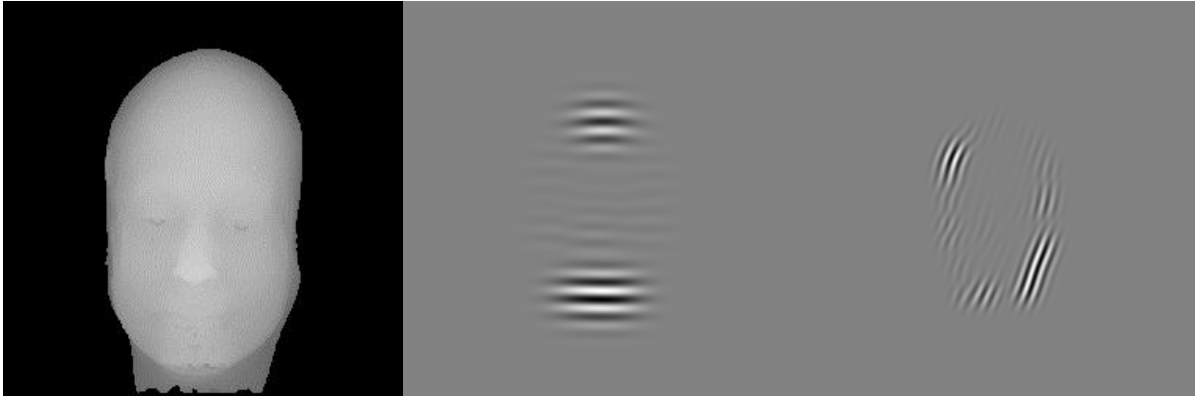


**Figure 2.** Original depth map and its convolutions with Gabor Wavelets with different orientation and scale

The second step in the process involved transforming the facial depth map into a space where features were more distinct from one another. An appropriate space is the Gabor space. A Gabor filter is a linear filter used for edge detection. Frequency and orientation representations of Gabor filters are similar to those of the human visual system, and they have been found to be particularly appropriate for texture representation and discrimination. Since the Gabor filter is very similar to the image processing performed in the human visual system, features in the resulting Gabor space are likely to have good correlation with features used by human observers. In the spatial domain, a 2D Gabor filter is a Gaussian kernel function modulated by a sinusoidal plane wave. In our work, we used Gabor wavelets, since they can be designed for a number of dilations and rotations, and a filter bank consisting of Gabor filters with various scales and rotations can be precomputed for improved performance. We used 5 different dilations and 8 different orientations resulting in 40 different wavelets. These wavelets are convolved with the signal, resulting in the Gabor space. (Figure 2 shows an example.)

The next step involved classifying features in the Gabor space. From the Gabor space we kept the values of the neighborhood of the feature for each of the 40 Gabor wavelets. Because of the small number of training cases available we used principal component analysis to reduce the feature set down to the 10 most significant eigenvectors. We used a neural network classifier with ten input nodes (one for each input value), a hidden layer with two nodes, and an output node. The network was trained using back propagation.

To speed up feature identification and avoid false positives, we restricted the search for features to a window around the shifted population average location for each feature in the training set. The population average location was shifted by the location of the closest point in the depth map, which we assumed was the tip of the nose. We examined three different widths for the search window. For each feature, we computed the average distance between the user specified feature locations and the shifted (by the computed nose location) population average locations. The maximum average displacement was nearly 16 pixels, so we set our default window width as 20 and compared this to window widths half (10) and twice (40) as wide.

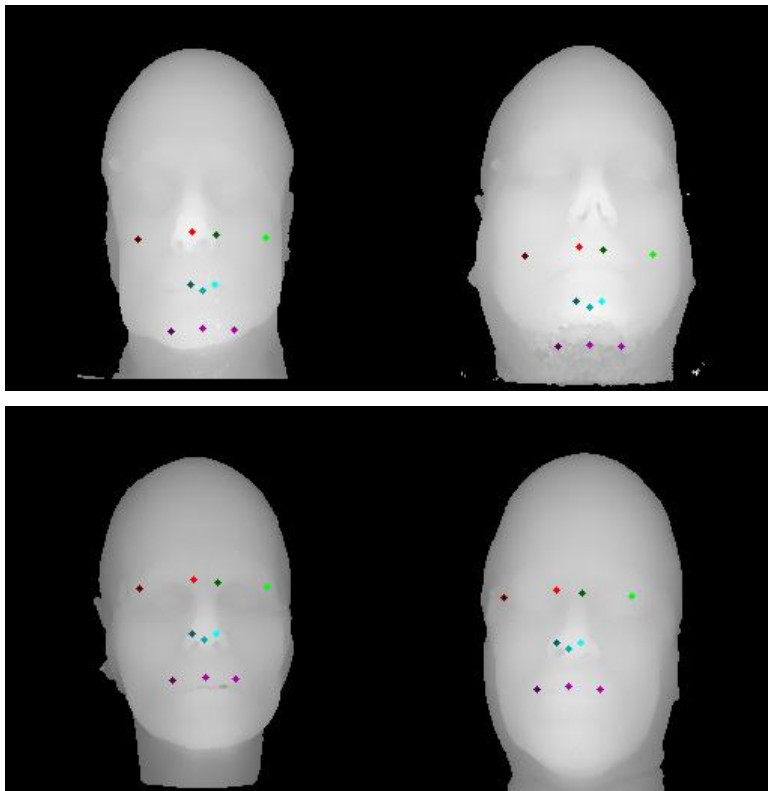


**Figure 3.** Example of the population-average location shifted by the detected bottom of the nose. In the top row, we show the two cases where the chin was incorrectly identified rather than the nose. In the bottom row we show two other cases randomly selected from the remaining 27 cases.

Twenty-nine manually annotated cases were used to train and evaluate the feature identification algorithm. We used a leave-one-out methodology where the neural networks were trained using the remaining 28 cases and tested against the one left out. The displacement between the manually marked features and the neural network detected features were measured.

## Results

Our assumption that the nose was the most forward coronal object was evaluated by visual inspection of the marked images. Our assumption held for 27 of the 29 cases, but failed for two cases. In one case noise resulted in an incorrect surface formation (Figure 4, top left). In the other case, the head was tilted and both the chin and nose extended beyond the field-of-view, and the chin was incorrectly selected (Figure 3, top right).

The mean (x,y) displacements for the 10, 20, and 40 pixel windows were (4.0,12.5), (7.0,12.4), and (11.2,12.7) pixels respectively. The displacement errors were similar for all features.

As an initial exploration of the usefulness of our feature detection for minimal de-facing, we built a minimal defacing algorithm based on the MRI defacing algorithm developed by Bischoff-Grethe et al. In this approach, the “face” is identified by the difference between the original image and the defaced image. The face is then minimally defaced by eliminating square regions in the coronal planes corresponding to the locations of the detected features. The modified face is then added back to the defaced image. An example of this is shown in Figure 4.

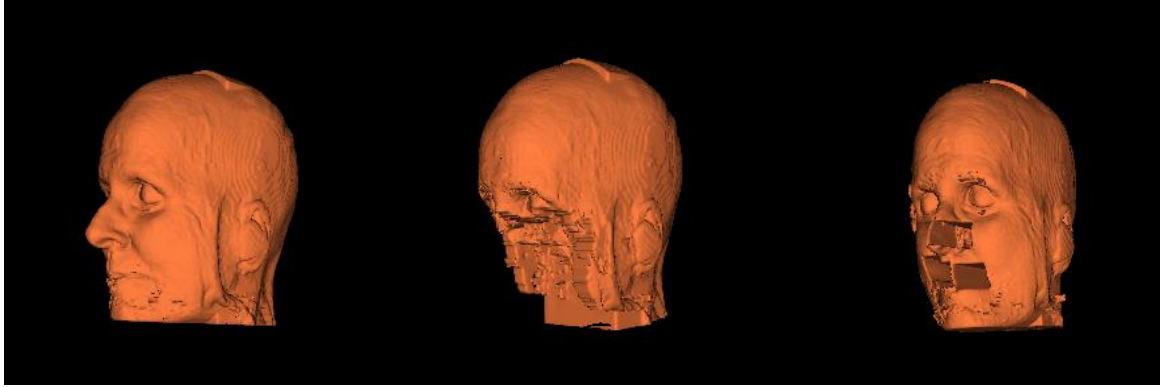


**Figure 4.** Example surface renderings of the original MR image (left), defaced image using the technique of Bischoff-Grethe et al (center), and a minimal defacing based on the feature detection described in this paper.

### Discussion

There are several limitations to our current work. First, we had a relatively small data set; the number of training cases for each feature was only approximately three, whereas a common rule-of-thumb is to have 10 data points for each feature. Second, we only concerned ourselves with coronal features, although the technique could easily be extended to other views to identify ears and jaw lines. Third, we treated each point feature as independent, whereas in reality these points are highly correlated. Our results would likely have been improved if we treated the features for each anatomic object (eye, nose, mouth) as line segments rather than as independent points, since the line properties such as length and orientation could have helped constrain the search. An illustration of this constraint problem is shown in Figure 5, where the detected right nostril and the detected bottom of the nose have the same x value and the middle of the mouth has a large y shift relative to left and right mouth features.

The results shown in Figure 4 are typical of the minimal defacing results we are currently getting, indicating that the feature detection is partly useful but requires more accurate placement of the features. Over an examination of multiple cases, our biggest difficulty seems to be with eliminating the eyes, which is a combination of both the misplacement of our own eye detection and the partial exclusion of the eye regions from the face in Bischoff-Grethe's technique.



**Figure 5.** Nose and mouth region for example case showing relative feature detection distortions.

An interesting observation is that our y variability (inferior/superior position) is much greater than that of our x variability. This is understandable in light of both the oval shape of the face and the positioning of patients in MR scanners. This suggests that in future work we should use rectangular rather than square search windows.

We presented a framework for minimal removal of identifiable features in structural head images. We plan to greatly expand our training set (the ADNI Alzheimer's database contains several hundred images), and to introduce constraints in the relative locations of the specified features, as discussed above to eliminate distortions in the spatial relationships between our detected features. The minimal defacing based on an improved algorithm will be validated using an observer performance experiment.

This work was funded by NIH Grant U54 HL108460.

### References

1. Bruce V, Henderson Z, Greenwood K, Hancock P, Burton AM, Miller P. Verification of face identities from images captured on video. *Journal of Experimental Psychology: Applied*. 1999;5:339-360.
2. Bowyer KW, Chang K, Flynn P. A survey of approaches and challenges in 3D and multi-modal 3D + 2D face recognition. *Computer Vision and Image Understanding* 2005;101:1-15.
3. Zhang Y, Xu S, Sun N. Skull recognition based on Embedded Hidden Markov models. *Intelligent Control and Automation. WCICA 7th World Congress*. 2008:1153-1158.
4. Bischoff-Grethe A, Ozyurt I, Busa E, et al. A technique for the deidentification of structural brain MR images. *Hum Brain Mapp* 2007;28:892-903.
5. Schimke N, Kuehler M, Hale J. Preserving Privacy in Structural Neuroimages. In Li Y. edited "Data and Applications Security and Privacy XXV." Springer LNCS 2011;6818: 301-308.
6. Weiner MW, Aisen PS, Jack CR Jr., et al. The Alzheimer's disease neuroimaging initiative: progress report and future plans. *Alzheimers Dement* 2010;6:202-11.